Journal of the European Ceramic Society **16** (1996) 1099–1106

PII: S0955-2219(96)00031-6
0955-2219/96/$15.00

Influence of the Oxygen Pressure on the Chemical State of Yttrium in Polycrystalline α-Alumina. Relation with Microstructure and Mechanical Toughness

M. K. Loudjani & C. Haut

Laboratoire de Métallurgie Structurale, CNRS URA 1107, bât.413, Université Paris XI, 91405 Orsay, France

(Received 15 November 1995; revised version received 16 January1996; accepted 23 January 1996)

Abstract

The influence of yttrium on the microstructure and toughness of α-alumina is studied as a function of oxygen partial pressure and chemical state of the doping element. For doping amounts higher than 0·03 mol% of Y_2O_3, $Y_3Al_5O_{12}$ garnet precipitates and the alumina grain size is then limited by such a precipitation along grain boundaries. For doping amounts lower than or equal to 0·03 mol% of Y_2O_3, yttrium ions are in solid solution as defect complexes of the type $(2Y'_{Al} + mV_O^{\cdot\cdot} + nO_i'')^{2(m-n)\cdot}$ and segregates along grain boundaries. The stability of the defect complexes is promoted by low oxygen pressures and the grain size is limited by the yttrium segregation along grain boundaries. At high oxygen pressures, the yttrium solubility decreases and an enrichment in yttrium is observed at the sample surface. Simultaneously, an abnormal alumina grain growth appears. The alumina toughness, estimated by indentation, is improved by the presence of defect complexes at low oxygen pressures while the $Y_3Al_5O_{12}$ garnet precipitates increase the alumina brittleness.

Nous avons étudié le rôle de l'yttrium sur la microstructure et sur la ténacité de l'alumine-α en relation avec la pression partielle d'oxygène et l'état chimique du dopant. Pour des teneurs en dopant plus grandes que 0,03% mol. Y_2O_3, l'yttrium précipite sous forme $Y_2Al_5O_{12}$, la taille de grains est alors limitée par la précipitation de cette phase aux joints de grains. Pour des teneurs ≤ 0,03% mol. Y_2O_3 l'yttrium est en solution solide et ségrège aux joints de grains. Dans cet état l'yttrium forme des défauts complexes du type $(2Y'_{Al} + mV_O^{\cdot\cdot} + nO_i'')^{2(m-n)\cdot}$ dont la stabilité est favorisée par les faibles pressions partielles d'oxygène. Dans ce cas, la taille de grains et leur grossissement anormal sont limités par la ségrégation de l'yttrium aux joints de grains. Les fortes pressions d'oxygène au contraire diminuent la solubilité de l'yttrium ce qui induit alors, après recuit un énrichissement de la surface des echantillons en yttrium provenant du coeur du matériau et un grossissement anormal des grains d'alumine. La ténacité de l'alumine a été évaluée par indentation: La ténacité de l'alumine est légèrement améliorée en présence de complexes de défauts introduits aux basses pressions d'oxygène alors que la phase durcissante $Y_3Al_5O_{12}$ rend le matériau plus fragile.

1 Introduction

Alumina is one of the most stoichiometric oxides and both its transport properties and its microstructure are strongly dependent on the amount of impurities present.

In the case of an intrinsic ceramic, the thermodynamic factors responsible for the creation of point defects during its elaboration are the temperature and the oxygen pressure. At high oxygen partial pressure, the promoted point defects consists of aluminium vacancies ($[V_{Al}'''] \propto (pO_2)^{3/16}$) and oxygen interstitials ($[O_i''] \propto (pO_2)^{1/6}$) whereas, at low oxygen pressure, the promoted point defects are the oxygen vacancies ($[V_O^{\cdot\cdot}] \propto (pO_2)^{-1/6}$) and the aluminium interstitials ($[Al_i^{\cdot\cdot\cdot}] \propto (pO_2)^{-3/16}$).

In the case of an extrinsic alumina doped by yttrium, studies by EXAFS of the local disorder around yttrium atoms and by electron diffraction[1–3] indicate that for yttrium contents greater than 300 ppm mol Y_2O_3, most of the yttrium is precipitated as yttrogarnet phase $Y_3Al_5O_{12}$, while for yttrium contents less than or equal to 300 ppm mol Y_2O_3, yttrium atoms are in solid solution in the polycrystalline alumina samples. This is shown schematically in Figs 1(a) and (b) where it appears that the Fourier

transformed spectra of 1 or 0·1 mol% Y_2O_3-doped Al_2O_3 are close to that of $Y_3Al_5O_{12}$ [Fig. 1(a)] while the spectrum related to 300 ppm mol Y_2O_3-doped Al_2O_3 is close to that of Al_2O_3 [Fig. 1(b)], indicating that yttrium ions (Y^{3+}) in solid solution are localized on cationic sites. The number of first neighbouring atoms around yttrium on aluminium sites ($N_1 \approx 3$, see Table 1) is lower than that around aluminium ions in alumina ($N_1 \approx 6$) or that in standard compounds such as Y_2O_3 and $Y_3Al_5O_{12}$, for which the coordination is equal to 6 or 8, respectively. Due to their great size, yttrium ions in solid solution induce oxygen lattice distortions:[1-3] around each yttrium ion 'm' oxygen vacancies ($V_O^{\cdot\cdot}$) are created

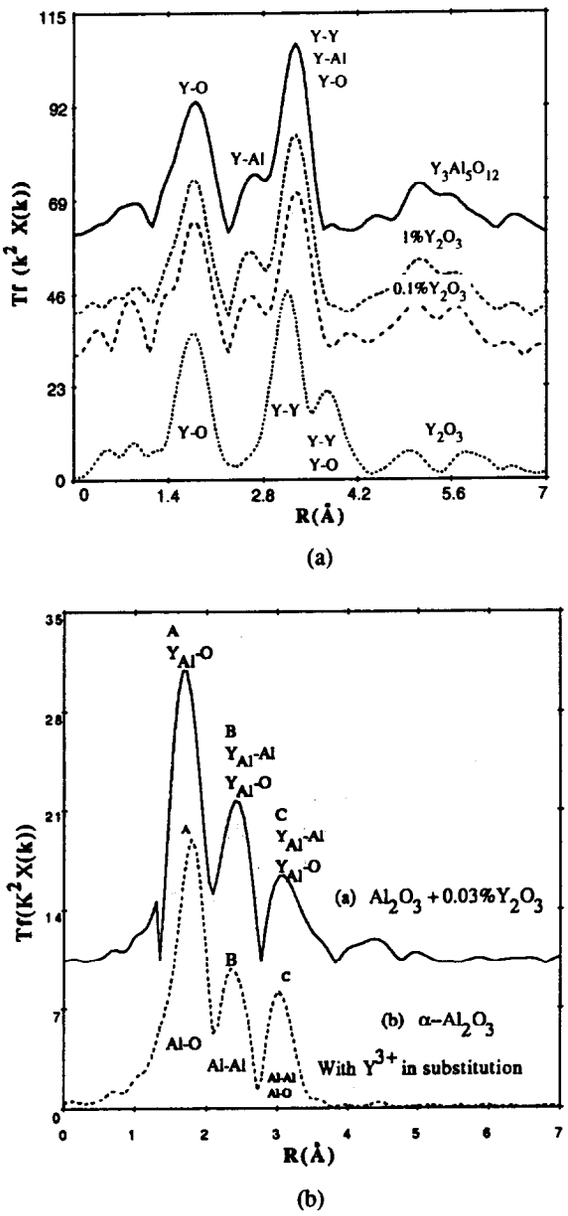

Fig. 1. (a) Fourier transform spectra (uncorrected for phase shift) of standards: $Y_3Al_5O_{12}$, Y_2O_3 and highly doped α-aluminas (1 mol% of Y_2O_3). (b) Fourier transform spectrum calculated for α-Al_2O_3 with dissolved yttrium ions located on aluminium sites (taking into account the size effect of yttrium ions with the creation of oxygen vacancies in the first shell of oxygen neighbouring species) and experimental spectrum for the 0·03 mol% Y_2O_3-doped α-alumina.

Table 1. Values of the parameters R_j(Å) and N_j for undoped alumina, and determined from the A and B peaks for the 0·03 mol% Y_2O_3 polycrystalline doped alumina [Fig. 1(b)]. R_j(Å) is the distance between neighbouring atoms and N_j is the number of neighbouring atoms

Sample	*Shell*	$\overline{R_j(Å)}$	$\overline{N_j}$
Al_2O_3	Y_{Al}–O	1·912	6
	Y_{Al}–Al	2·755	4
	Y_{Al}–Al	3·403	9
	Y_{Al}–O	3·405	9
0·03 mol% Y_2O_3	<Y–O>1	2·325 ± 0·08	2·7 ± 0·5
	<Y–Al>2	2·741 ± 0·08	2·6 ± 1
	<Y–O>3	2·845 ± 0.08	1·7 ± 1

with $m \approx 2{\cdot}7$, and 'n' oxygen interstitials appear in a second intermediate shell with $n \approx 1{\cdot}7$. This corresponds to the creation of defect complexes which can be written as:

$$3O_O + 2Y_{Al}^{x} \Leftrightarrow (2Y_{Al}^{x} + mV_O^{\cdot\cdot} + nO_i'')^{2(m-n)\cdot} + \frac{3-n}{2} O_2 + 2(m-n)e' \text{ with } m > n \quad (1)$$

with $m > n$. Thus, the concentration of the defect complex $(2Y_{Al}^{x} + mV_O^{\cdot\cdot} + nO_i'')^{2(m-n)\cdot}$ depends on the oxygen pressure.

Observations and analyses by transmission electron microscopy have suggested that most of the yttrium is segregated along grain boundaries.[1,3] Segregation phenomena and the amount and nature of the point defects in a ceramic such as alumina are very important for most of its properties, particularly for transport and mechanical properties or for the protective character of alumina scales developed on former alumina alloys. Thus it is important to relate the microscopic defects (point defects, segregation, etc.) to the macroscopic properties of alumina. In the first part of this work, the effect of yttrium doping on the microstructure of α-alumina will be presented, and the influence of oxygen pressure on the amount and nature of the point defects and on segregation phenomena will be analysed. In the second part, the evolution of alumina toughness as a function of the microstructure and the chemical state of yttrium will be presented and discussed.

2 Experimental Procedure

2.1 Materials and heat treatments

Several α-aluminas, either without or with yttrium doping corresponding to 1, 0·1 and 0·03 mol% Y_2O_3,[3,4] were prepared by powder sintering carried out under secondary vacuum in a graphitic crucible ($pO_2 \approx 10^{-13}$ atm).[5] The microstructural observations were made on five types of sample: as-sintered samples ($pO_2 \approx 10^{-13}$ atm); and samples heat-treated

at either 1400 or 1650°C for times varying between 15 min to 75 h, then air-quenched.

The heat treatments were performed either in air in an alumina crucible or at low oxygen pressure via CO gas ($pO_2 \approx 10^{-16}$ atm at 1650°C). In the case of heat treatments in a reducing atmosphere, in order to avoid carbon contamination the samples were placed first in a alumina crucible which, in turn, was placed in a closed graphitic crucible.

2.2 Microstructural observations and image analyses

The sample microstructure was observed by scanning electron microscopy (SEM) with backscattered electrons on a digitalized Stereoscan Leica 260 SEM equipped with an energy-dispersive X-ray analysis (EDAX) system. Image treatment was conducted via OPTILAB software from Graftek. It is first necessary to reproduce the sample surface microstructure obtained from backscattered electrons on tracing paper. Such plots are then transformed via an optical camera into binary images which are then transferred to the computer to be analysed.

Complementary data were obtained by chemical analyses performed on thin foils by transmission electron microscopy (TEM) equipped with scanning tunnelling electron microscopy (STEM) device and an EXDS system. Such a technique was used especially for the α-alumina doped with 0·03 mol% Y_2O_3.

2.3 Toughness measurements

In order to characterize the ceramic toughness and the effect of yttrium doping, indentation tests were performed in macrohardness mode with a load of 1 kg and in microhardness mode with a load of 200 g, using a Vickers indentor. This technique, first proposed by Evans and Charles,[6] allows a quick determination of the toughness of small samples of ceramic materials.[6–9] In the conditions used, the imprints have an average size of about 30 μm with the macrohardness mode and 15 μm with the microhardness mode. The relations enabling the Vickers hardness H_v and the toughness K to be calculated are:

$$H_v = 1{\cdot}8544 \frac{Pg}{(2a)^2}$$

and

$$K = 0{\cdot}014 \left(\frac{E}{H_v}\right)^{1/2} \frac{Pg}{c^{3/2}}$$

where P is the applied load, g is the acceleration due to gravity, $2a$ is the imprint diameter, E is the Young's modulus of the material and $2c$ is the radial crack length. Measurement of the crack length ($2c$) and the imprint size ($2a$) was performed by optical and scanning electron microscopies.

3 Results and Discussion

3.1 Morphology of samples heat-treated in air at 1400 or 1650°C

Grain size distribution plots were established on a population of about 1300 grains at 1400 and 1650°C. As an example, Fig. 3 shows the grain size distribution as a function of the amount of yttrium dopant (0, 0·03 and 1 mol% of Y_2O_3) and duration of the heat treatment (1, 24 and 72 h) at 1400°C, in air. Simultaneously, observations of the sample surface by SEM (Fig. 4) indicate that, whatever the temperature and duration of the heat treatment in air, the grain size of highly doped alumina samples (1 mol% of Y_2O_3) is smaller than that of other alumina samples (undoped or 0·03 mol% of Y_2O_3). In the highly doped samples, the grain size and the distribution of the precipitated second phase ($Y_3Al_5O_{12}$) are homogeneous on all the sample, whatever the heat treatment temperature [Fig. 4(a)]. In contrast, for the weakly doped samples [particularly for 0·03 mol% of Y_2O_3, Fig. 4(b)], there is heterogeneous grain size distribution with an abnormal grain growth. Such an analysis indicates that the amount of yttrium necessary to avoid the abnormal grain growth during heat treatments in air at high temperature is around 1 mol% Y_2O_3.

The results of a kinetic study on the surface segregation of yttrium associated with precipitation of the yttrogarnet phase $Y_3Al_5O_{12}$ at 1400 and 1650°C are collected in Fig. 5 for the density of precipitates according to their surfaces and in Fig. 6 for the microstructure in the case of α-alumina doped with 0·03 mol% Y_2O_3 as an example. Whatever the temperature and the yttrium content, the amount of $Y_3Al_5O_{12}$ phase at the alumina surface increases with time. This indicates that a dynamic segregation occurring during cooling can be excluded and that the precipitation of yttrogarnet results from an equilibrium segregation. The relative proportion of the $Y_3Al_5O_{12}$ phase localized along grain boundaries

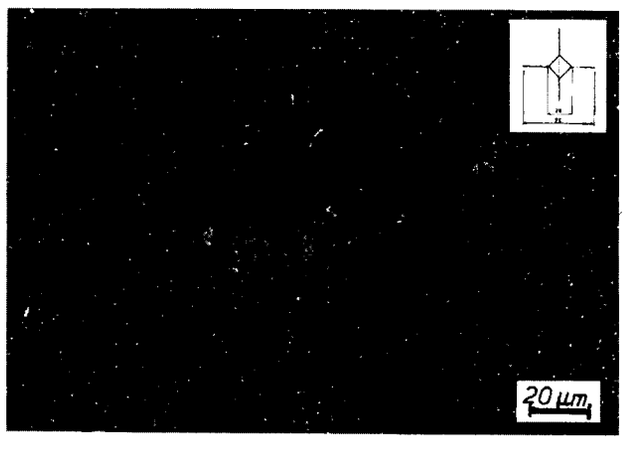

Fig. 2. Micrograph and scheme of Vickers indentation on doped α-Al_2O_3 (1 mol% Y_2O_3), showing the radial crack extension.

and in the bulk of the grains (Fig. 5) varies with time, and the ratio $[Y_3Al_5O_{12}]_{gb}/[Y_3Al_5O_{12}]_{bulk}$ decreases with heat treatment duration from about 8 after 1 h to about 2 after 72 h of treatment. For a treatment at 1650°C and for the same duration (72 h), the amount of $Y_3Al_5O_{12}$ precipitates along grain boundaries is

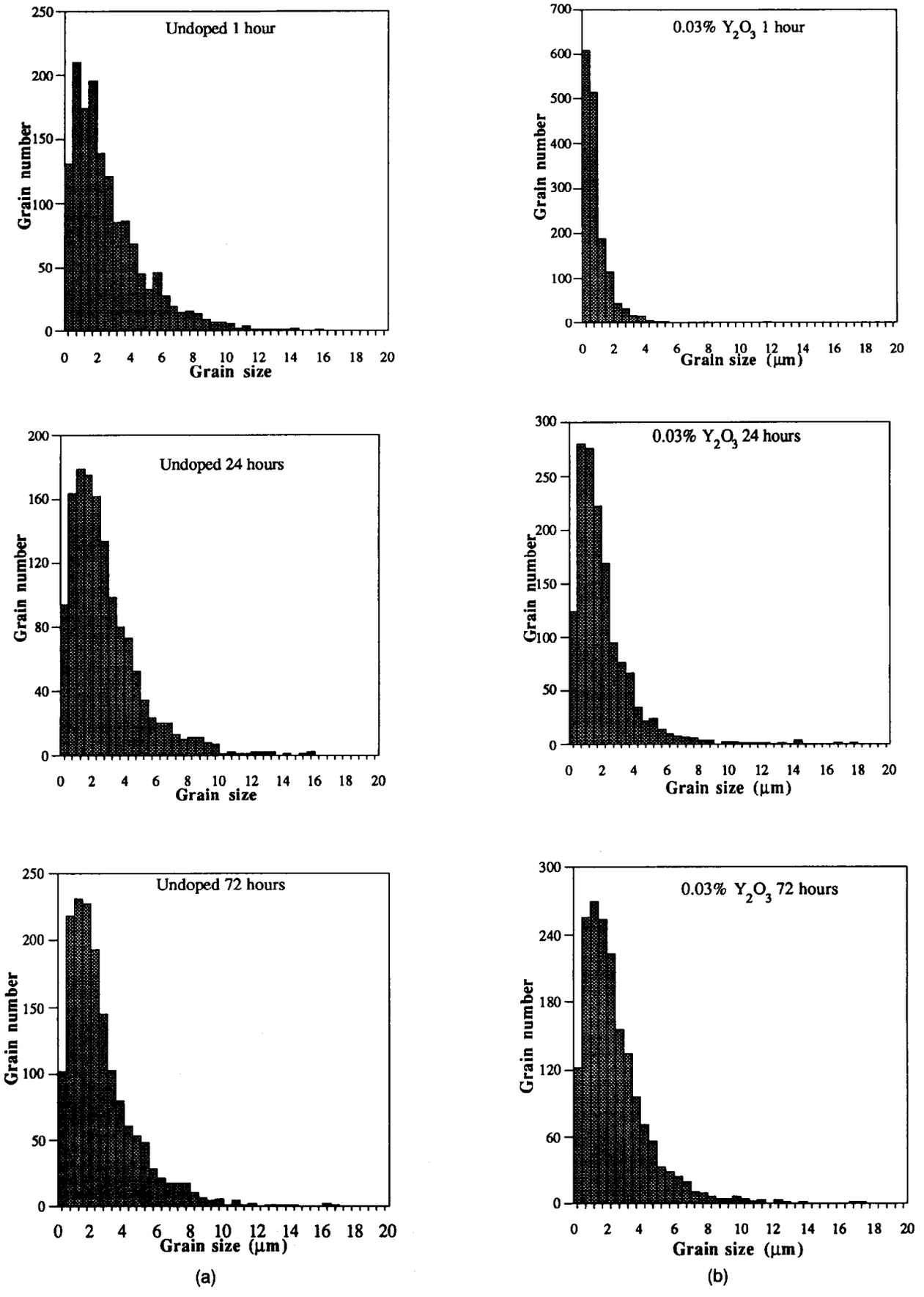

Fig. 3. Distribution of the grain size of undoped alumina (a) 300 ppm yttrium-doped alumina (b) and 1 mol% Y_2O_3-doped alumina (c) samples as a function of the heat treatment duration at 1400°C in air.

three times greater than the amount of yttrogarnet precipitates in the bulk of the grains due to the grain size variation with temperature.

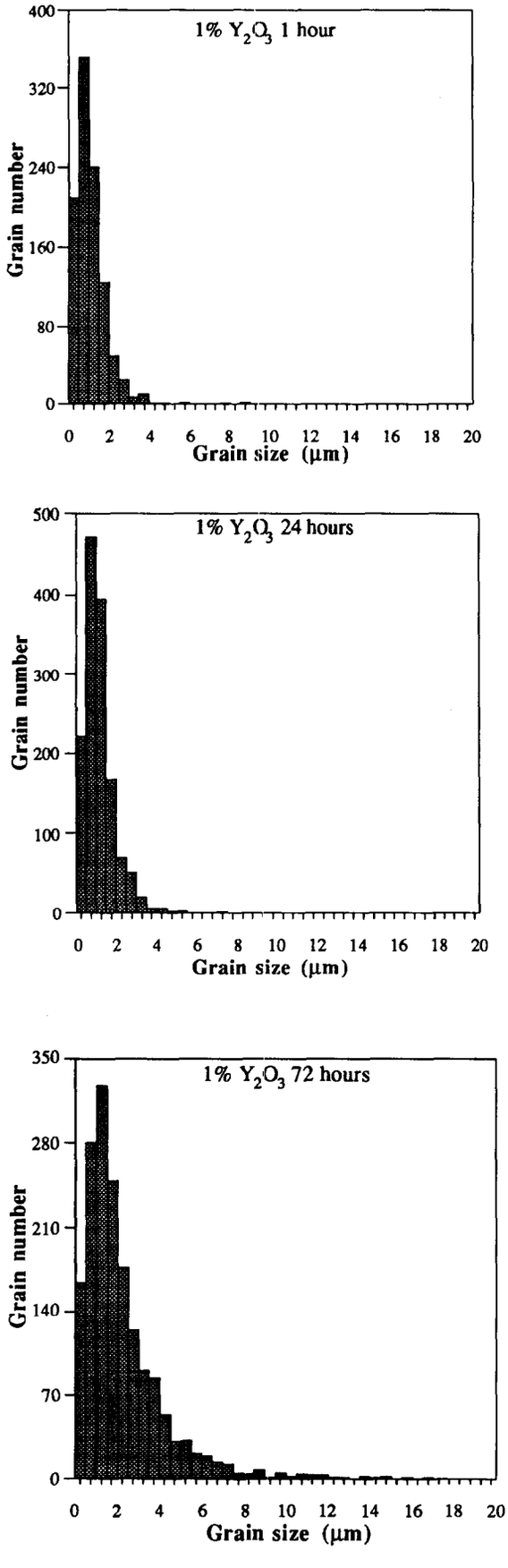

(c)

Fig 3. Continued

3.2 Influence of oxygen partial pressure on the microstructure of α-alumina doped with 0.03 mol% Y_2O_3

Chemical analyses of thin foils by TEM were performed on alumina samples doped with 0·03 mol% Y_2O_3. On as-sintered samples (i.e. elaborated at a low oxygen pressure, $pO_2 \approx 10^{-13}$ atm, see section 2.1), the analyses show an important increase of the yttrium concentration towards grain boundaries (Fig. 6). The amount of yttrium along grain boundaries C_{gb} is greater than the amount of yttrium in the bulk C_b, and the concentration ratio $C_{gb}/C_b \approx 50$. However, on samples heat-treated in air at 1650°C, no yttrium segregation or precipitation is observed along grain boundaries.

SEM observations of weakly doped samples (0·03 mol% Y_2O_3) heat-treated in a reducing atmosphere of CO can be compared with the microstructures obtained in air (compare Figs 4(b) and 7). The micrographs indicate that the morphology of the grain boundaries and the grain size are different, depending on the oxygen partial pressure during heat treatment. For the samples heat-treated in air [Fig. 4(b)] a bimodal distribution of the grain size is

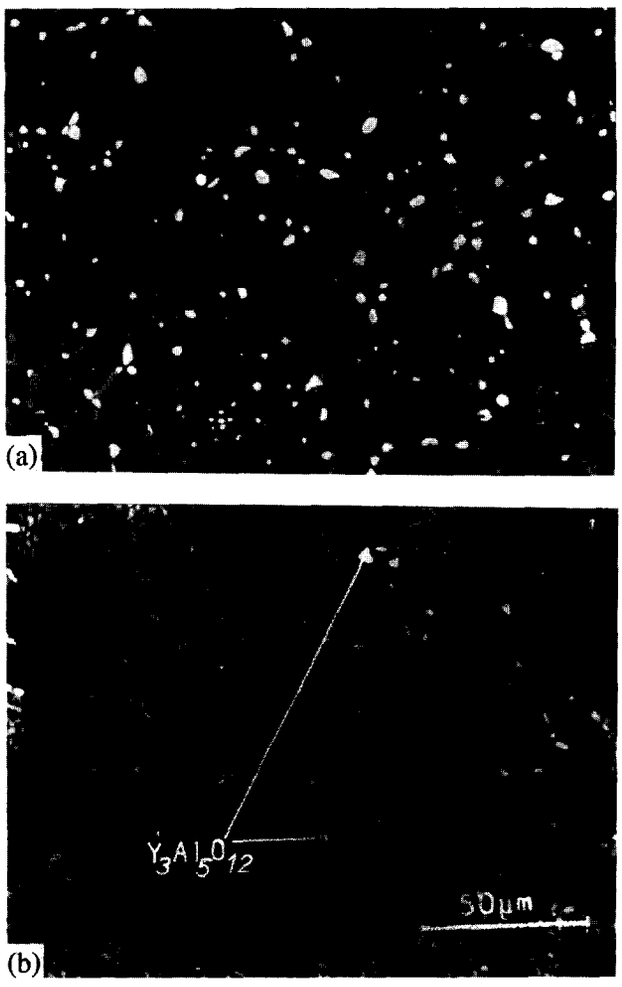

Fig. 4. Influence of yttrium on the microstructure of samples heat-treated for 24 h at 1650°C in air. White particles are $Y_3Al_5O_{12}$ (arrow), average size = 1·8–2·6 μm. (a) 1 mol% of Y_2O_3-doped sample; (b) 0.03 mol% Y_2O_3-doped sample.

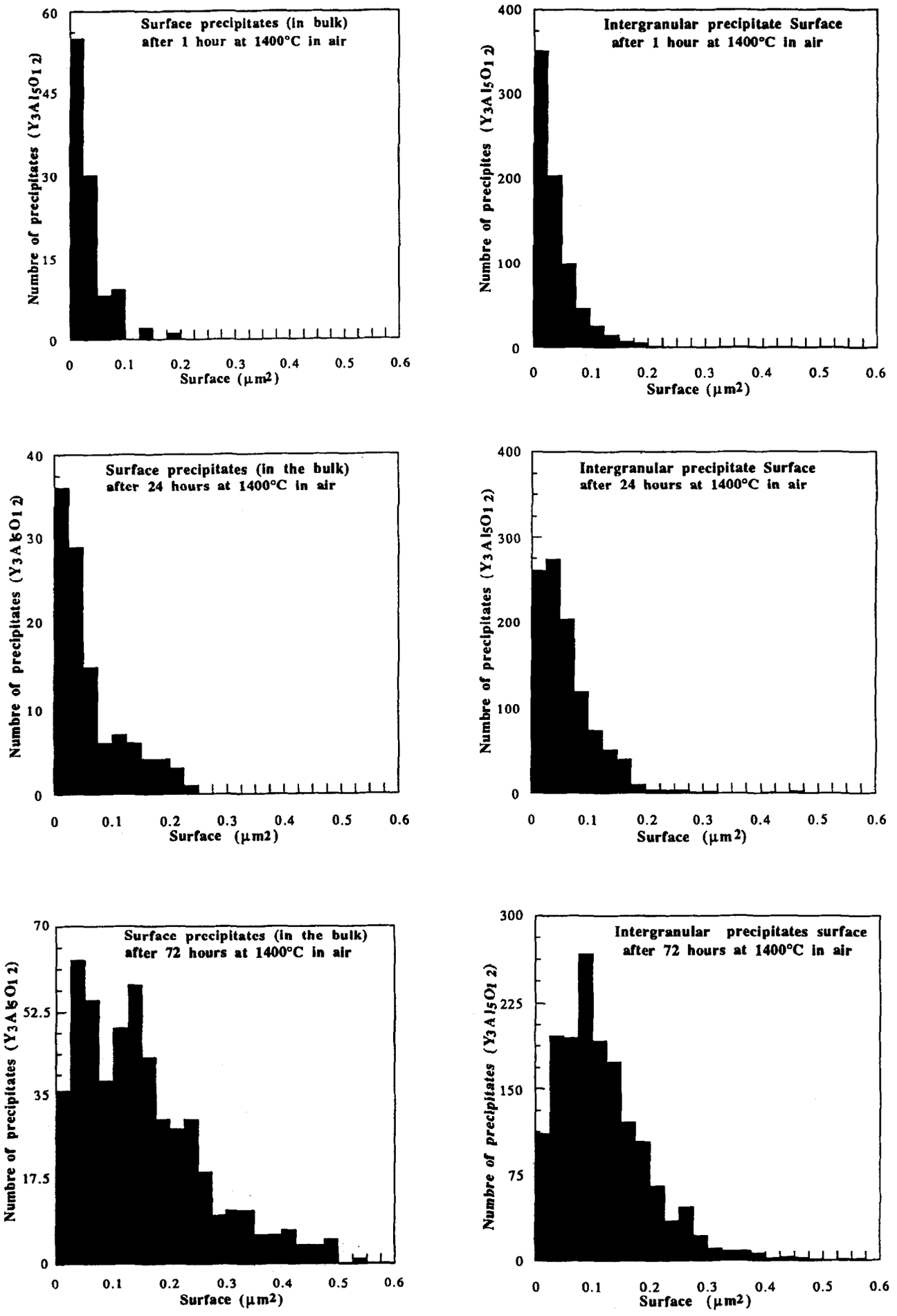

Fig. 5. Density of the yttrogarnet precipitates according to their surface versus the duration of the heat treatment in air at 1400°C. (a) Precipitates localized along grain boundaries; (b) precipitates localized in the bulk of the grains.

observed: some of the grains have a small size (1–5 μm) while others can reach 140 μm (abnormal growth). Simultaneously, the amount of $Y_3Al_5O_{12}$ precipitates at the sample surface increases with heat treatment duration (cf. Fig. 6). In contrast, for samples heat-treated in CO (Fig. 7) the number of garnet precipitates at the sample surface is negligible and the grain size distribution is homogeneous: most of the grains have a size between 4 and 15 μm. These observations indicate that the yttrium solubility in the bulk of the α-alumina samples is greater at low oxygen pressure than at high pO_2 The yttrium segregation along grain boundaries (cf. Fig. 6) hinders both the segregation at the surface and the abnormal grain growth which are observed after heat treatment in air. This means that the yttrium draining from the sample bulk towards the sample surface during heat treatment in air is due to the driving force related to the concentration gradient of point defects such as oxygen vacancies or interstitials ($V_O^{\cdot\cdot}$, O_i'') from the bulk to the surface:[10–13]

$$F_C \propto kT\frac{\Delta C}{C}$$

The diffusion of these defects is the origin of the yttrium segregation associated with the precipitation of $Y_3Al_5O_{12}$ at the sample surface.

3.3 Toughness

The variation of the toughness of the samples as a function of the yttrium content is reported in Fig. 8 for as-sintered samples [Fig. 8(a)] and for samples heat-treated for 24 h at 1400°C in air [Fig. 8(b)]. The average values of toughness obtained in this work are of the same order of magnitude as those given by Mckinney *et al.*[9] for polycrystalline commercial alumina but somewhat higher than those determined on single crystals by Evans and Charles.[6] In our case, it can be observed that heat treatments

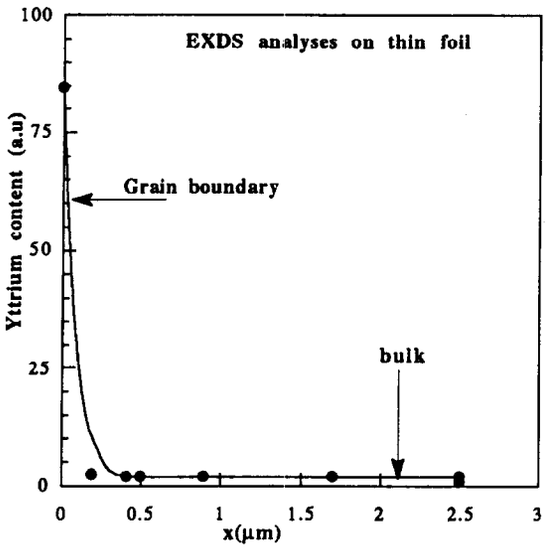

Fig. 6. STEM analyses on thin foils of as-sintered α-alumina doped with 0·03 mol% of Y_2O_3, showing the evolution of the $L\alpha_Y$ X-ray emission from a grain boundary to the bulk.

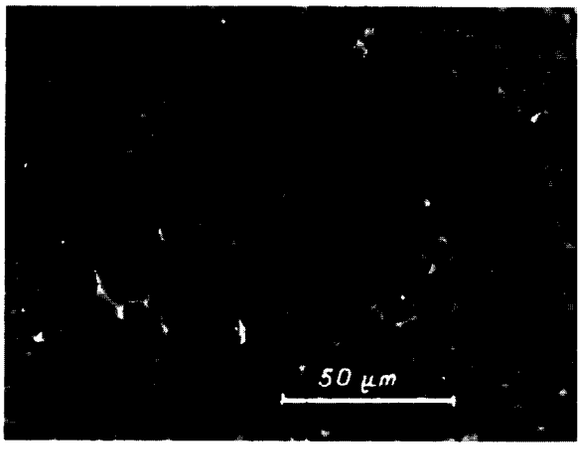

Fig. 7. Microstructure of 0·03 mol% Y_2O_3-doped alumina heat-treated in a CO atmosphere (in carbon graphite crucible) at 1650°C for 24 h.

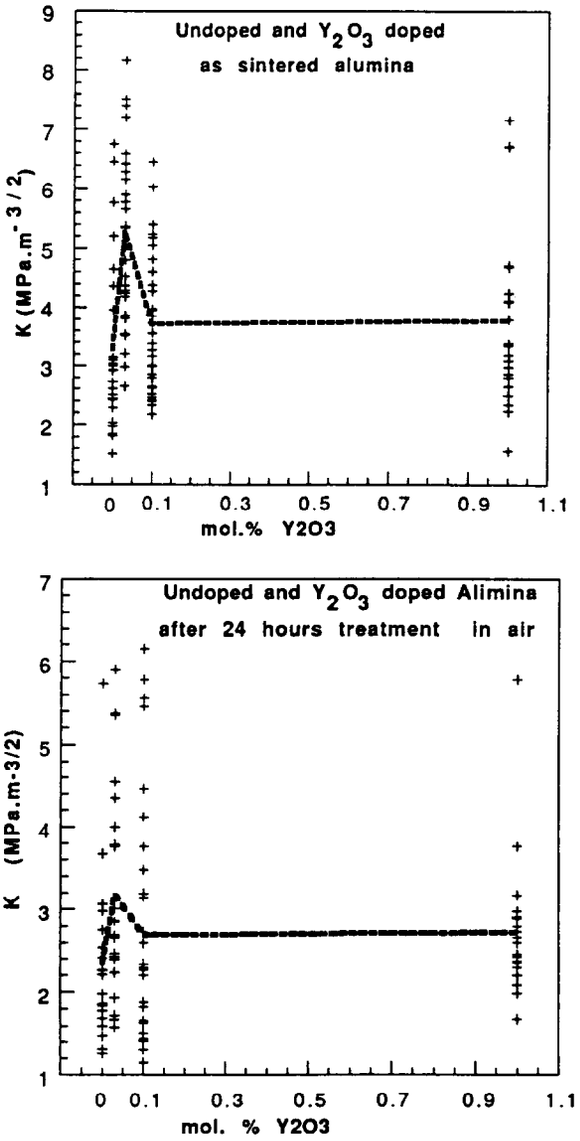

Fig. 8. Variations of toughness as a function of yttrium doping amount. (a) As-sintered samples (treatment in a reducing atmosphere); (b) samples heat-treated in air for 24 h at 1400°C. (+) Experimental points, line represents average value.

in air lead to slightly smaller average toughness values than when the alumina samples are heat-treated in CO atmosphere. Moreover, independent of the atmosphere (air or CO), the toughness variations go through a maximum value for the weakly doped samples (0·03 mol% of Y_2O_3). Thus the toughness seems to be more dependent on the stoichiometry and the microchemistry of the samples (point defects, yttrium grain boundary segregation) than on the alumina macrostructure (grain size, heterogeneous distribution of the garnet precipitates). Indeed, in the case of the as-sintered alumina samples doped with 300 ppm Y_2O_3, yttrium ions in solid solution in the bulk or segregated along grain boundaries (see Fig. 6) lead to the generation of defect complexes according to eqn (1). This type of defect seems to improve the mechanical properties of alumina. After a heat treatment in air, the amount of $Y_3Al_5O_{12}$ precipitates at the sample surface increases significantly and simultaneously a decrease of the toughness is observed whatever the material may be.

4 Conclusion

A study of the microstructure and toughness of polycrystalline α-aluminas doped with various amounts of yttrium and heat-treated either in reducing atmosphere or in air leads to the following results.

(1) In alumina, the amount of yttrium necessary to avoid grain growth of the garnet phase is about 1 mol% of Y_2O_3.
(2) The yttrium solubility increases when the oxygen pressure decreases.
(3) At low oxygen pressure, the abnormal grain growth is less important than at high oxygen pressure. This is related to the yttrium segregation along grain boundaries which is promoted at low pO_2. This phenomenon corresponds to an equilibrium segregation.
(4) The mechanical properties of α-alumina are improved when yttrium is either in solid solution or segregated along grain boundaries. Precipitation of the $Y_3Al_5O_{12}$ phase decreases the alumina toughness, whereas, in contrast, the toughness is improved by the presence of structural defects introduced during the elaboration (point defects, grain boundary segregation).

Acknowledgements

The authors are indebted to A. M. Huntz and P. Carry, Institut de Science des Matériaux, Orsay, for fruitful discussions, to P. Carry for providing sintered aluminas and to S. Parisot for her help with the experimental work.

References

1. Loudjani, M. K., Huntz, A. M. & Cortès, R., Influence of yttrium on microstructure and point defect in α-Al_2O_3. Relation with oxidation. *J. Mater. Sci.*, **28** (1993) 6466–6473.
2. Loudjani, M. K. & Cortès, R., X-ray absorption study of the local structure and the chemical state of yttrium in polycrystalline α-alumina. *J. Eur. Ceram. Soc.*, **13** (1994) 77.
3. Loudjani, M. K., Thèse de Docteur d'Etat, Université Paris XI, Orsay, France, 1992.
4. Loudjani, M. K., Lesage, B. & Huntz, A. M., Influence du dopage et du mode d'élaboration sur la microstructure de l'alumine-α polycristalline — relation avec les propriétés de transport. *Industrie Céramique*, **801** (1986) 53.
5. Sato, E. & Carry, C., Sintering and yttrium grain boundary segregation in sub-micron size alumina. *J. de Phys. IV, Colloque C7*, **3** (1993) 1335.
6. Evans, A. G. & Charles E. A., Fracture toughness determinations by indentation. *J. Am. Ceram. Soc.*, **59**[7] (1976) 371.
7. Lawn, B. R., Evans, A. G. & Marshall D. B., Elastic plastic indentation damage in ceramics. The median radial cracks system. *J. Am. Ceram. Soc.*, **63**[9] (1980) 574.
8. Cook, R. F. & Pharr, G. M., Direct observation and analysis of indentation cracking in glasses and ceramics. *J. Am. Ceram. Soc.*, **73**[4] (1990) 787.
9. Mckinney, K. R., Chaskelis, H. H. & Freiman, S. W., Prediction of flaw sizes from acoustics emission measurement in ceramics. *J. Am. Ceram. Soc.*, **59**[7] (1976) 369.
10. Mackrodt, W. C., The calculated equilibruim segregation of Fe^{3+}, Y^{3+}, and La^{3+} at the low index surfaces of α-Al_2O_3. *Adv. Ceram.*, **23** (1987) 247.
11. Mackrodt, W. C. & Tasker, P. W., Segregation isotherms at the surfaces of oxides. *J. Am. Ceram. Soc.*, **72**[9] (1989) 1576.
12. Petot-Ervas, G. & Petot, C., Point defects and mass transport under a thermodynamic potential gradient, *J. Phys. Chem. Solids*, **51** (1990) 901.
13. Monceau, D., Petot-Ervas, G. & Petot, C., Kinetic demixing profile calculation in oxide solid solutions under chemical potential gradient. *Solid State Ionics*, **45**, (1990), 231.